JOC*Article*

Modeling S_N2 Reactions in Methanol Solution by ab Initio Calculation of Nucleophile Solvent−Substrate Clusters

Xufeng Lin,[†] Cunyuan Zhao,[‡] and David Lee Phillips*,[†]

Department of Chemistry, University of Hong Kong, Pokfulam Road, Hong Kong, P. R. China, and School of Chemistry and Chemical Engineering, Sun Yat-Sen University, Guangzhou 510275, P. R. China

phillips@hkucc.hku.hk

Received June 22, 2005

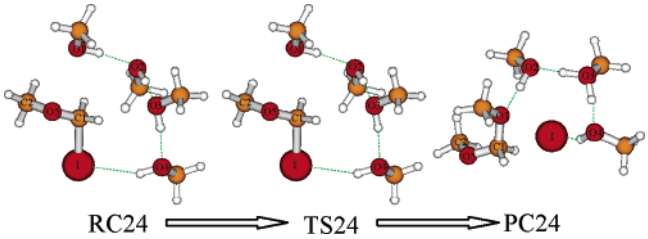

Ab initio calculations were used to study the S_N2 reactions of the CH_3OCH_2I molecule with a methoxide ion (CH_3O^-) and a methanol molecule by systematically building up the reaction system with explicit incorporation of the methanol solvent molecules. For the reaction of CH_3OCH_2I with a methoxide ion, the explicit incorporation of the methanol molecules to better solvate the methoxide ion led to an increase in the barrier to reaction. For the reaction of CH_3OCH_2I with a methanol molecule, the explicit incorporation of the methanol molecules led to a decrease in the barrier to reaction because of an inclination of this reaction to proceed with the nucleophilic displacements accompanied by proton transfer through the H-bonding chain. The H-bonding chain served as both acid and base catalysts for the displacement reaction. A ca. 10^{15}-fold acceleration of the methanol tetramer incorporated S_N2 reaction was predicted relative to the corresponding methanol monomer reaction. The properties of the reactions examined are discussed briefly.

Introduction

Bimolecular nucleophilic substitution (S_N2) reactions are an important class of organic reactions that have been widely investigated experimentally and theoretically.[1−13] Anion−molecule (X^- + RY) and molecule−molecule (X + RY) displacements are two important types of S_N2 reactions. For the anion−molecule displacement reactions, the energy diagrams in the gas phase exhibit a double-well character.[1−4,6] The two minima are due to a reactant complex and a product complex that lie among the separated reactants, the transition state, and the separated products. In the solution phase, the anion is often better solvated in the reactant complex than in the transition state where the charge on the anion transfers partly along the X → R → Y direction. This often leads to an increase in the activation energy as the reaction system becomes better solvated. So, the anion−molecule displacement type of S_N2 reaction can be much faster in the gas phase than in the solution phase.[6,7] These reactions may also become much faster in dipolar aprotic solvents than in protic solvents.[8] Bohme and Baksit[9] constructed microsolvated nucleophiles $RO^{-\bullet}(ROH)_n$ (R = H, CH_3, CH_2CH_3, and $CH(CH_3)_2$) to investigate S_N2 reactions with monohalomethane in a flowing solvent and

[†] University of Hong Kong.
[‡] Sun Yat-Sen University.

(1) Carroll, F. A. In *Perspectives on structure and mechanism in organic chemistry*; Brook/Cole Publishing Co.: CA, 1998.
(2) Olmstead, W. N.; Brauman, J. I. *J. Am. Chem. Soc.* **1977**, *99*, 4219.
(3) Chandrasekhar, J.; Jorgensen, W. L. *J. Am. Chem. Soc.* **1985**, *107*, 2974.
(4) Chabinyc, M. L.; Craig, S. L.; Regan, C. K.; Brauman, J. L. *Science* **1998**, *279*, 1882.
(5) (a) Hase, W. L. *Science* **1994**, *266*, 998. (b) Sun, L.; Song, K.; Hase, W. L. *Science* **2002**, *296*, 875.
(6) Vayner, G.; Houk, K. N.; Jorgensen, W. L.; Brauman, J. I. *J. Am Chem. Soc.* **2004**, *126*, 9054.
(7) Tanaka, K.; Mackay, G. I.; Payzant, J. D.; Bohme, D. K. *Can. J. Chem.* **1976**, *54*, 1643.
(8) Parker, A. J. *Chem. Rev.* **1969**, *69*, 1.
(9) Bohme, D. K.; Raksit, A. B. *J. Am. Chem. Soc.* **1984**, *106*, 3447.
(10) Morokuma, K. *J. Am. Chem. Soc.* **1982**, *104*, 3732.
(11) Zhao, X. G.; Lu, D. H.; Liu, Y. P.; Lynch, G. C.; Truhlar, D. G. *J. Chem. Phys.* **1992**, *97*, 6369.
(12) Tucker, S. C.; Truhlar, D. G. *J. Am. Chem. Soc.* **1990**, *112*, 3447.
(13) (a) Yamataka, H.; Aida, M. *Chem. Phys. Lett.* **1998**, *289*, 105. (b) Aida, M.; Yamataka, H. *J. Mol. Struct.: THEOCHEM* **1999**, *461−462*, 417.

10.1021/jo051280+ CCC: $30.25
Published on Web 10/19/2005

H_2 gas with controlled temperature and pressure. Theoretical calculations demonstrated that, for the $Cl^-\cdot(H_2O)$ reaction with CH_3Cl, the transition states were stabilized less than those for the Cl^- reaction.[10−14] Computations on similar microsolvated systems for solvents other than H_2O are not common. Compared to the anion−molecule type of nucleophilic displacement reactions, there are even fewer computational studies reported in the literature for the molecule−molecule displacement S_N2 reactions.

Alcohols (ROH) are important nucleophiles in organic chemistry and in some biological systems. For example, the hydrolysis of ester or amide substrates catalyzed by serine proteases undergoes nucleophilic attack with serine hydroxyl.[15] Previous computational studies[16−20] on water/methanol-catalyzed dehydrohalogenation reactions indicate that additional water/methanol molecules help stabilize the leaving group. For the molecule−molecule displacement type of reaction, the solvation of the neutral nucleophiles will also likely help stabilize the transition states that have more ionic character than the reactants. Ab initio calculations that explicitly build up the microsolvated system can help to better understand the role of individual solvent molecules in the solvation of the reaction system. These calculations can also provide important clues for understanding the solvation effect on these anion−molecule and molecule−molecule types of S_N2 reactions in protic solvents.

In this paper, we report ab initio calculations for nucleophilic anion−molecule and molecule−molecule displacement reactions for iodoether in methanol solvent. The unsolvated/solvated nucleophiles are denoted as $CH_3O^-\cdot(CH_3OH)_n$ (n = 0, 1, 2, and 3) and $(CH_3OH)_n$ where n = 1, 2, 3, and 4, respectively, and they react with iodoether by the respective reactions 1 or 2:

$$CH_3OCH_2I + CH_3O^- + (CH_3OH)_n \rightarrow CH_3OCH_2OCH_3 + I^- + (CH_3OH)_n \quad (1)$$

where n = 0, 1, 2, and 3 respectively, and

$$CH_3OCH_2I + (CH_3OH)_n \rightarrow CH_3OCH_2OCH_3 + HI + (CH_3OH)_{n-1} \quad (2)$$

where n = 1, 2, 3, and 4, respectively.

For reaction 1, the explicit incorporation of the methanol molecules to better solvate the CH_3O^- ion resulted in an increase in the barrier to reaction. For reaction 2, the explicit incorporation of the methanol molecules resulted in a decrease in the barrier to reaction because of the nucleophilic displacements being accompanied by proton transfer through the H-bonding chain, which served as both acid and base catalysts for the displacement reaction. A ca. 10^{15}-fold acceleration was found for the methanol tetramer incorporated S_N2 reaction 2 (e.g., $CH_3OCH_2I + (CH_3OH)_4 \rightarrow CH_3OCH_2OCH_3 + HI + (CH_3OH)_3$) relative to the corresponding methanol monomer reaction (e.g., $CH_3OCH_2I + CH_3OH \rightarrow CH_3OCH_2OCH_3 + HI$). Reactions 1 and 2 are compared to each other and discussed as a function of the number of methanol molecules involved in the reaction. The possible implications for anion−molecule and molecule−molecule S_N2 reactions occurring in methanol solution are briefly discussed.

Computational Methods

The potential energy surfaces (PES) of CH_3OCH_2I reacting with methanol-solvated methoxide ions and methanol clusters were explored by optimizing the structures of the reactant complexes (RC), transition states (TS), and product complexes (PC) for the reactions of interest. RC*mn*, TS*mn*, and PC*mn* denote the structures obtained from the calculations where *m* (=1 and 2) is number of the reaction examined and *n* (=0, 1, 2, and 3) is the number of additional CH_3OH molecules incorporated into the reaction systems. For example, RC12 is the reactant complex of reaction 1 with two additional CH_3OH molecules and TS23 is the transition state of reaction 2 with three CH_3OH molecules. The geometry optimization and frequency analysis were performed at the MP2 level of theory with the Gaussian 98 suite of programs (A7 version).[21] Two levels of basis sets were used in this work, and they are denoted as BS1 and BS2. In the BS1 basis set, the 6-31G* basis set was used for the C and H atoms, the 6-31+G* basis set was used for the O atom, and the lanl2dz basis set with a d polarization of 0.266 was used for I the atom.[22] To obtain more accurate thermodynamic data for reaction 2, we have performed single-point MP2 computation with the BS2 basis set, where the aug-cc-PVDZ basis set was used for the C, H, and O atoms and the 6-311G** basis set was used for the I atom. Five component d functions were employed in the whole calculation. From the energy and free-energy data shown in Table 4, we see that the results obtained from the MP2/BS1 and MP2/BS2 calculations are rather close to each other. The MP2/aug-cc-pvdz results in Table 5 are also consistent with results for the G3MP2 method,[21b] which is an accurate method for thermodynamic computations. These results indicate that the MP2/BS1 calculations are probably adequate for the systems of interest here. The Cartesian coordinates, the total energies, and the selected output from the calculations for all of the calculated structures are provided in the Supporting Information. Intrinsic reaction coordination (IRC) computations were done to confirm the transition states connected the appropriate reactants and products.[23]

(14) Okuno, Y. *J. Am. Chem. Soc.* **2000**, *122*, 2925.
(15) Fersht, A. In *Structure and mechanism in protein science*; W. H. Freeman and Company: New York, 1999.
(16) (a) Kwok, W. M.; Zhao, C. Y.; Guan, X. G.; Li, Y. L.; Du, Y.; Phillips, D. L. *J. Chem. Phys.* **2004**, *120*, 9017. (b) Kwok, W. M.; Zhao, C.; Li, Y. L.; Guan, X.; Wang, D.; Phillips, D. L. *J. Am. Chem. Soc.* **2004**, *126*, 3119.
(17) Zhao, C. Y.; Lin, X. F.; Kwok, W. M.; Guan, X. G.; Du, Y.; Wang, D. Q.; Hung, K. F.; Phillips, D. L. *Chem.−Eur. J.* **2005**, *11*, 1093.
(18) Phillips, D. L.; Zhao, C. Y.; Wang, D. Q. *J. Phys. Chem. A* **2005**, *109*. ASAP DOI:10.1021/jp053015y.
(19) Lin, X. F.; Guan, X. G.; Kwok, W. M.; Zhao, C. Y.; Du, Y.; Li, Y. L.; Phillips, D. L. *J. Phys. Chem. A* **2005**, *109*, 981.
(20) (a) Lin, X. F.; Zhao, C. Y.; Phillips, D. L. *Chem. Phys. Lett.* **2004**, *397*, 488. (b) Guan, X. G.; Lin, X. F.; Kwok, W. M.; Zhao, C. Y.; Du, Y.; Phillips, D. L. *J. Phys. Chem. A* **2005**, *109*, 1247.
(21) (a) Frisch, M. J.; Trucks, G. W.; Schlegel, H. B.; Scuseria, G. E.; Robb, M. A.; Cheeseman, J. R.; Zakrzewski, V. G.; Montgomery, J. A., Jr.; Stratmann, R. E.; Burant, J. C.; Dapprich, S.; Millam, J. M.; Daniels, A. D.; Kudin, K. N.; Strain, M. C.; Farkas, O.; Tomasi, J.; Barone, V.; Cossi, M.; Cammi, R.; Mennucci, B.; Pomelli, C.; Adamo, C.; Clifford, S.; Ochterski, J.; Petersson, G. A.; Ayala, P. Y.; Cui, Q.; Morokuma, K.; Malick, D. K.; Rabuck, A. D.; Raghavachari, K.; Foresman, J. B.; Cioslowski, J.; Ortiz, J. V.; Stefanov, B. B.; Liu, G.; Liashenko, A.; Piskorz, P.; Komaromi, I.; Gomperts, R.; Martin, R. L.; Fox, D. J.; Keith, T.; Al-Laham, M. A.; Peng, C. Y.; Nanayakkara, A.; Gonzalez, C.; Challacombe, M.; Gill, P. M. W.; Johnson, B. G.; Chen, W.; Wong, M. W.; Andres, J. L.; Head-Gordon, M.; Replogle, E. S.; Pople, J. A. *Gaussian 98*; Gaussian, Inc.: Pittsburgh, PA, 1998. (b) Curtiss, L. A.; Redfern, P. C.; Raghavachari, K.; Rassolov, V.; Pople, J. A. *J. Chem. Phys.* **1999**, *110*, 4703.
(22) Huzinaga, S.; Anzelm, J.; Klobukowski, M.; Radzio-Andzelm, E.; Sakai, Y.; Tatewaki, H. In *Gaussian Basis Sets for Molecular Calculations*; Elsevier: Amsterdam, 1984.

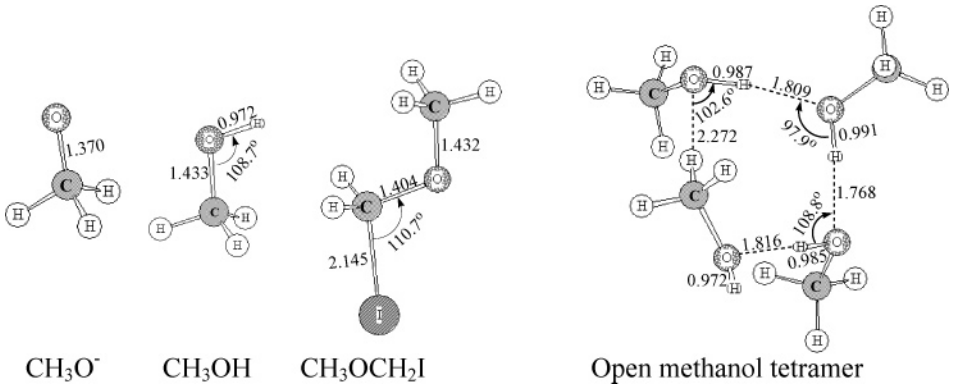

FIGURE 1. Simple schematic diagrams showing the optimized structures for all the separated reactants (CH_3O^-, CH_3OH, and CH_3OCH_2I) and open methanol tetramers obtained at the MP2/BS1 level of theory.

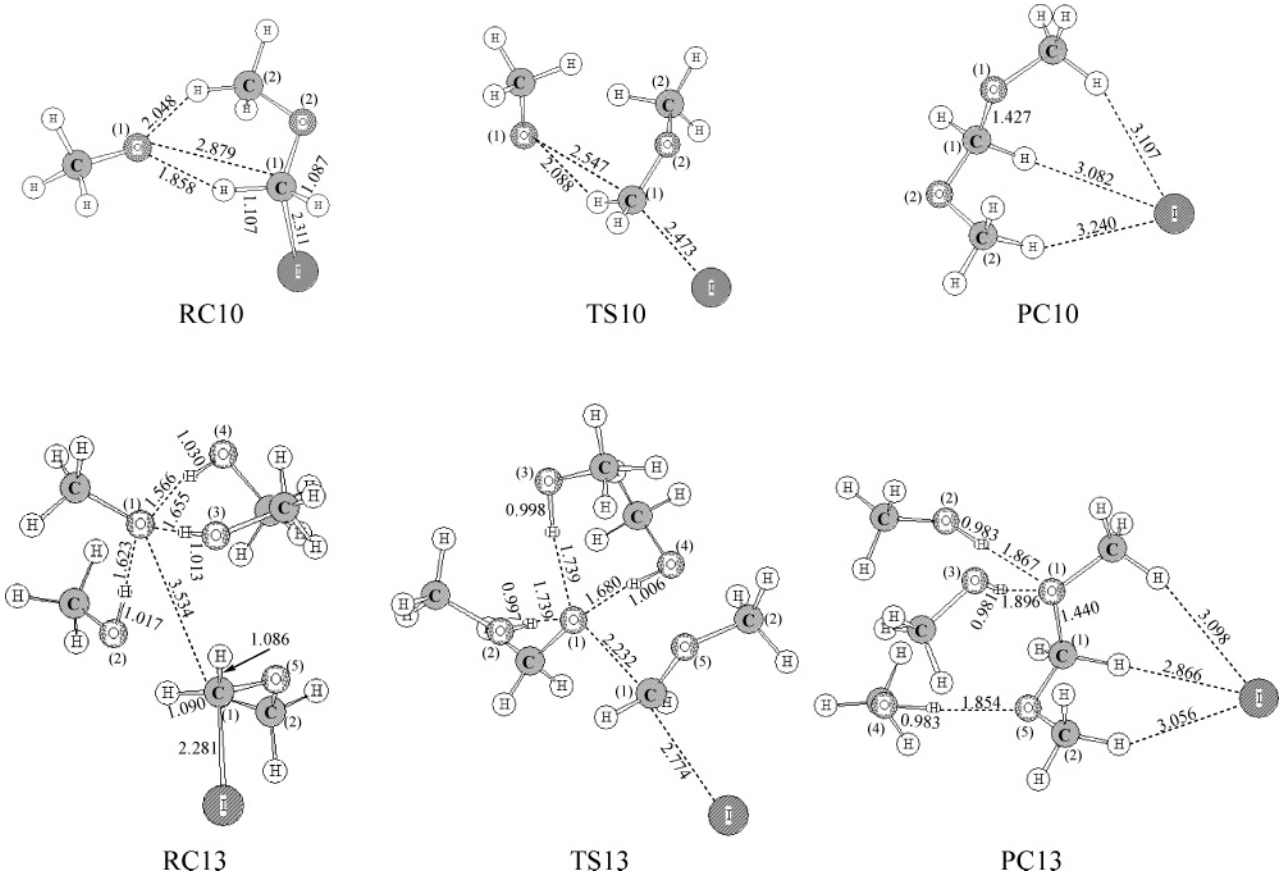

FIGURE 2. Simple schematic diagrams of the optimized structures obtained from the MP2/BS1 ab initio calculations for the reactant complexes, transition states, and product complexes of the reactions of $CH_3OCH_2I + CH_3O^- + (CH_3OH)_n \rightarrow CH_3OCH_2OCH_3 + I^- + (CH_3OH)_n$ where $n = 0$ and 3. Structures for $n = 1$ and $n = 2$ can be seen in Figure S2 in the Supporting Information. See text for more details.

Results and Discussion

A. Reactions of $CH_3O^-\cdot(CH_3OH)_n$ with CH_3OCH_2I. Figure 1 presents the optimized structures for the separated reactants (CH_3O^-, CH_3OH, and CH_3OCH_2I) and the open methanol tetramer $(CH_3OH)_4$ obtained at the MP2/BS1 level of theory. Figure S1 in the Supporting Information shows the optimized structures for all the separated reactants and methanol-solvated methoxide ion complexes, $CH_3O^-\cdot(CH_3OH)_n$ (n = 1, 2, and 3), and methanol clusters, $(CH_3OH)_n$ (n = 1, 2, 3, and 4), obtained at the MP2/BS1 level of theory. Figure 2 presents the optimized geometries at the MP2/BS1 level of theory for all of the reactant complexes (RCs), transition states (TSs), and product complexes (PCs) for reaction 1. Figure 3 depicts the MP2 computed relative energies (in kcal/mol with zero-point energy correction) for the starting materials, RCs, TSs, and PCs.

The formation of the reactant complexes leads to a significant increase in the C(1)−I bond length compared

(23) (a) Gonzalez, C.; Schlegel, H. B. *J. Chem. Phys.* **1989**, *90*, 2154−2161. (b) Gonzalez, C.; Schlegel, H. B. *J. Phys. Chem.* **1990**, *94*, 5523−5527.

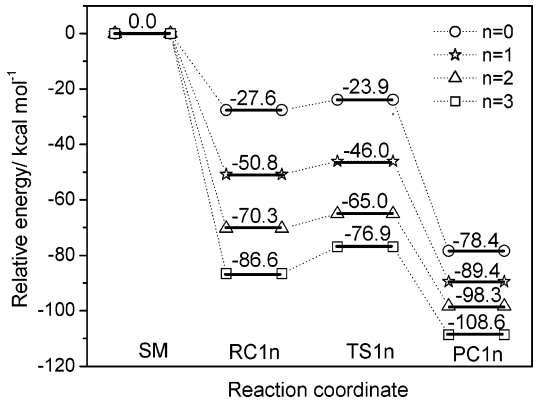

FIGURE 3. Schematic diagram depicting the MP2/BS1 calculated relative energies (in kcal/mol) for selected key reactants, transition states, and products for the reactions of $CH_3OCH_2I + CH_3O^- + (CH_3OH)_n \rightarrow CH_3OCH_2OCH_3 + I^- + (CH_3OH)_n$ where $n = 0$, 1, 2, and 3. See text for more details.

to that in the free CH_3OCH_2I (2.153 Å) molecule. The C(1)−I bond length decreases somewhat as the number of methanol molecules increases. The C(1)−H bond length is longer than the normal C−H bond because of the strong C(1)H···O interaction. The elongation of the C(1)−H bonds decreases when more CH_3OH molecules are incorporated into the RCs, from 1.107 Å in RC10 to 1.090 Å in RC13. This suggests that the interaction between CH_3OCH_2I and the methoxide/solvated-methoxide ions decreases as one goes from RC10 to RC13, which will be discussed in more detail later. The C(1)···O(1) distance becomes longer in the RCs with an increasing number of CH_3OH molecules in the system, from 2.879 Å in RC10 to 3.534 Å in RC13. From the structure of RC13, we can see that the methoxide ion is almost surrounded by the CH_3OH solvent molecules. The stabilization energy of the reactant complexes varies from −27.6 kcal/mol for RC10 to −86.6 kcal/mol for RC13. From the stabilization energies of $CH_3O^-\cdot(CH_3OH)_n$ ($n = 0$, 1, 2, and 3), we can further estimate the interaction energy between the solvated ion $CH_3O^-\cdot(CH_3OH)_n$ and the CH_3OCH_2I molecule. These energies are listed in Table 1. The methanol−methanol interaction energy is defined as $E_{Me-Me} = E_{CH_3O^-\cdot(CH_3OH)_n} - (E_{CH_3O^-} + nE_{CH_3OH})$. The methanol−iodoether interaction energy is defined as $E_{Me-iodoether} = E_{RC1n} - (E_{CH_3OCH_2I} + E_{CH_3O^-\cdot(CH_3OH)_n})$. The total stabilization energy is defined as $E_{total-stab} = E_{RC1n} - (E_{CH_3OCH_2I} + E_{CH_3O^-} + nE_{CH_3OH})$.

From Table 1, it was found that the interaction between the solvated anion and the iodoether molecule becomes weaker as the anion is better solvated (from 27.6 kcal/mol for $n = 0$ to 18.7 kcal/mol for $n = 3$). As the RCs proceed to their respective TSs, the trend of the geometry changes is clear as the number of methanol molecules increases in the reaction system. The TSs in Figure 2 display a typical trigonal bipyramidal geometry with respect to the O(1) attack and I leaving atoms. The C(1)···O(1) distance goes from 2.879 Å in RC10 to 2.547 Å in TS10, and the C(1)···I distance goes from 2.311 Å in RC10 to 2.473 Å in TS10. In the case of TS11, the C(1)···O(1) distance decreases to 2.349 Å and the C(1)···I distance increases to 2.600 Å. This indicates that the transition state comes later as one more methanol molecule is incorporated into the reaction system. The C(1)···O(1) distances in TS12 and TS13 become further shortened to 2.287 and 2.232 Å, respectively, and the C(1)···I distances become further enlongated to 2.648 and 2.774 Å, respectively. This leads to larger geometric differences between the RCs and their TSs, which implies that the reaction probably becomes more difficult as the reaction system is better solvated. The relative-energy diagrams for reaction 1 presented in Figure 3 also support this hypothesis. The activation energy increases from 3.7 kcal/mol for $n = 0$ to 9.7 kcal/mol for $n = 3$. All of the transition states found can proceed to the product complex of the diether and iodide anions that are shown as PC1n in Figure 2.

TABLE 1. MP2/BS1 Computed Stabilization Energies[a] for Methanol-Solvated CH_3O^- and Their Interaction with CH_3OCH_2I[b]

	$n = 0$	$n = 1$	$n = 2$	$n = 3$
$E_{CH_3O^-}$ (hartree)		−114.698		
nE_{CH_3OH} (hartree)	0	−115.300	−230.600	−345.900
$E_{CH_3O^-\cdot(CH3OH)n}$ (hartree)	−114.698	−230.041	−345.376	−460.706
E_{Me-Me} (kcal/mol)	0	27.3	49.0	67.9
$E_{CH_3OCH_2I}$ (hartree)		−165.111		
E_{RC1n} (hartree)	−279.853	−395.190	−510.521	−625.847
$E_{Me-iodoether}$	−27.6	−23.5	−21.3	−18.7
$E_{total-stab}$ (kcal/mol)	−27.6	−50.8	−70.3	−86.6

[a] With the correction of ZPE. [b] Note: $E_{Me-Me} = E_{CH_3O^-\cdot(CH_3OH)_n} - (E_{CH_3O^-} + nE_{CH_3OH})$, $E_{Me-iodoether} = E_{RC1n} - (E_{CH_3OCH_2I} + E_{CH_3O^-\cdot(CH_3OH)_n})$, $E_{total-stab} = E_{RC1n} - (E_{CH_3OCH_2I} + E_{CH_3O^-} + nE_{CH_3OH})$.

Comparison between the RCs and TSs from $n = 0$ to $n = 3$ reveals that the O−H bond lengths in the solvent methanol molecules decrease as one goes from the RCs to the TSs and that the H···O distances for the H bonding increase. The H bonding contributes mainly to the solvation energy in protic solvents. So, the geometrical changes in the H···O distance and O−H bond lengths indicate that there is a stronger interaction between the methoxide ion and solvent methanol molecules in the RCs than in the TSs. This suggests that the reaction complexes are better solvated by the additional CH_3OH molecules than are the transition states. For the anion−molecule S_N2 reaction, the charge on the nucleophile X^- goes along the X···C···Y axis to the leaving group Y.[1] It is useful to perform a charge-distribution analysis to better understand this process. The results of natural bond orbital (NBO) analysis of the RCs, TSs, and PCs are shown in Table 2.

The charge on the approaching O atom in RC10 is −1.112, which decreases to −1.083 for RC11 and then to −1.051 for RC13. This may indicate that the nucleophilicity of the CH_3O^- ion decreases as it is better solvated. The charge on the C(1) atom in the transition states becomes increasingly positive, and the charge on the I atom in the transition states becomes increasingly negative. Inspection of the charge difference between the reactant complexes and transition states, $(Q_{TS} - Q_{RC})_{O(1)}$, $(Q_{TS} - Q_{RC})_I$, and $(Q_{TS} - Q_{RC})_{C(1)}$, which are also listed in Table 2, shows that $(Q_{TS} - Q_{RC})_I$ and $(Q_{TS} - Q_{RC})_{C(1)}$ increase obviously from $n = 0$ to $n = 3$ and that $(Q_{TS} -$

TABLE 2. NBO Charges on the Approaching O(1) Atom, Leaving the I Atom, and the Center C(1) Atom for the Reaction 1 from the MP2/BS1 Computations

O(1)	$n = 0$	$n = 1$	$n = 2$	$n = 3$
reactant complex (RC)	−1.112	−1.083	−1.067	−1.051
transition state (TS)	−1.083	−1.059	−1.040	−1.039
product complex (PC)	−0.731	−0.742	−0.772	−0.772
$Q_{TS} - Q_{RC}$	0.029	0.024	0.027	0.012
$Q_{PC} - Q_{TS}$	0.352	0.317	0.268	0.267
I	$n = 0$	$n = 1$	$n = 2$	$n = 3$
reactant complex (RC)	−0.258	−0.224	−0.213	−0.193
transition state (TS)	−0.480	−0.619	−0.659	−0.754
product complex (PC)	−0.971	−0.963	−0.961	−0.958
$Q_{TS} - Q_{RC}$	−0.222	−0.395	−0.446	−0.561
$Q_{PC} - Q_{TS}$	−0.491	−0.344	−0.302	−0.204
C(1)	$n = 0$	$n = 1$	$n = 2$	$n = 3$
reactant complex (RC)	−0.028	−0.044	−0.037	−0.044
transition state (TS)	0.168	0.282	0.310	0.367
product complex (PC)	0.339	0.330	0.336	0.338
$Q_{TS} - Q_{RC}$	0.196	0.326	0.347	0.411
$Q_{PC} - Q_{TS}$	0.171	0.148	0.026	−0.029

$Q_{RC})_{O(1)}$ does not change much. These results indicate that during the attack of CH_3O^-, when the RCs go to their TSs, the charge transfer mainly takes place in the C(1)···I moiety and only a minor charge transfer occurs from O(1) to C(1). The larger value for the charge transfer between C(1)···I is possibly related to the decrease in the nucleophilicity of CH_3O^- as it is better solvated. As the TSs proceed to the PCs, the charges on the O(1) atoms decrease significantly, and this suggests that the charge transfer between the O(1)···C(1) part of the reaction system comes later than that between the C(1)···I part of the reaction system.

B. Reactions of $(CH_3OH)_n$ with Iodoether. The methanol clusters discussed in this section are shown in the Supporting Information, Figure S1. Figure 4 presents the optimized geometries of the RCs, TSs, and PCs of the reactions of $(CH_3OH)_n$ with iodoether (reaction 2), and Figure 5 shows alternative structures of RC23 and RC24 (denoted as RC23′ and RC24′) obtained from calculations using the BS2 basis set. Figure 6 depicts the MP2 calculated relative energies of the reactants, RCs, TSs, and PCs of reaction 2.

The nucleophilic attack of the carbon center of the iodoether by the methanol monomer has a reaction barrier of 37.2 kcal/mol ($\Delta G^{\ddagger}_{21}$ is 38.8 kcal/mol) at the MP2/BS1 level of theory. This indicates the reaction rate via RC21 has a rate constant of about 2×10^{-16}. This may be due to the poor nucleophilicity of methanol compared with that of the methoxide ion. Inspection of the first panel in Figure 4 shows that the formation of the reactant complexes leads to the elongation of the C(1)−I bond length. The C(1)···O(1) distance goes from 3.134 Å in RC21 to 2.351 Å in TS21, and the C(1)···I distance goes from 2.204 Å in RC21 to 3.375 Å in TS21. The O(1)−H bond length changes slightly from 0.976 Å in RC21 to 0.974 Å in TS21. In PC21, the H atom is completely detached from O(1) and the H−I bond is completely formed.

NBO analysis results in Table 3 reveal that, as RC21 goes to TS21, the charge of O(1) changes slightly (from −0.859 to −0.867) and that the charge of C(1) and the leaving I atom change dramatically, from −0.165 to 0.510 and from 0.004 to −0.871, respectively. This indicates that in the reaction coordinate of O(1)···C(1)···I the charge transfer mainly occurs on the C(1)···I moiety, and the energy barrier mainly comes from the cleavage of the C(1)−I bond. The charge on the C(1) atom in TS (0.510) is close to that of a free carbonium $CH_3OCH_2^+$ (0.525). This suggests that the iodoether reacts with the methanol monomer by a mechanism close to a S_N1 reaction or a very late S_N2 reaction. The diether $CH_3OCH_2OCH_3$ and the HI are formed as indicated in PC21. The $|Q_{PC} - Q_{TS}|_{O(1)}$ (=0.128) is close to $|Q_{PC} - Q_{TS}|_{C(1)}$ (=0.155), which indicates that the charge transfer from O(1) to C(1) occurs mainly as TS21 goes to PC21.

Addition of one methanol molecule to the reaction system can significantly catalyze this reaction by lowering the $\Delta E^{\ddagger}$ about 10 kcal/mol, as shown in Figure 6. The methanol dimer interacts with iodoether through H bonding in RC22, and the C(1)−I bond length is larger compared to that in RC21. As RC22 goes to TS22, O(1) attacks C(1) with a distance of 1.979 Å and the C(1)−I bond partially breaks to give a C(1)···I distance of 3.112 Å in TS22. This indicates that the nucleophilic displacement in TS22 is tighter than that in TS21.[1] Accompanying these changes, the O(2)H···I distance becomes shorter, from 2.780 Å in RC22 to 2.502 Å in TS22. The lengths of the two O−H bonds increase and the H···O distances of H bonding decrease. These changes lead to a six-membering character in TS22; i.e., the nucleophilic displacement is accompanied by the H transfer through the H-bonding chain. The product produced from TS22 shows a zwitterionic character, $(CH_3OH_2^+\cdots I)$,[16−20] where the O(2)H···I distance is 2.026 Å. Inspection of the NBO analysis results (in Table 3) shows that for the $n = 2$ case the charge on O(1) changes more significantly from RC22 to TS22 than that for the $n = 1$ case, accompanied with the charge on C(1) changing from −0.083 to 0.420 and the charge on I changing from −0.114 to −0.841. These charge changes indicate that charge transfer from O(1) to C(1) and from C(1) to I is more simultaneous for $n = 2$ than that for the $n = 1$ case. The charge on C(1) in TS22 (0.420) differs apparently from that on $CH_3OCH_2^+$. All these changes indicate that CH_3OCH_2I reacts with the methanol dimer through a more characteristic S_N2 process. The smaller $(Q_{TS} - Q_{RC})_I$ and $(Q_{PC} - Q_{TS})_I$ indicate that the second methanol molecule can stabilize the leaving I atom and/or is served as a general acid catalyst for the leaving I atom.

The H transfer accompanying the nucleophilic attack may also be achieved through a longer H-bonding chain and prompted us to further explore reaction 2 with larger methanol oligomers. Figure 6 shows that the energy barriers for CH_3OCH_2I reacting with the methanol trimer and tetramer are 18.1 and 14.9 kcal/mol, respectively, indicating that longer methanol chains are more efficient catalysts for the nucleophilic attack.

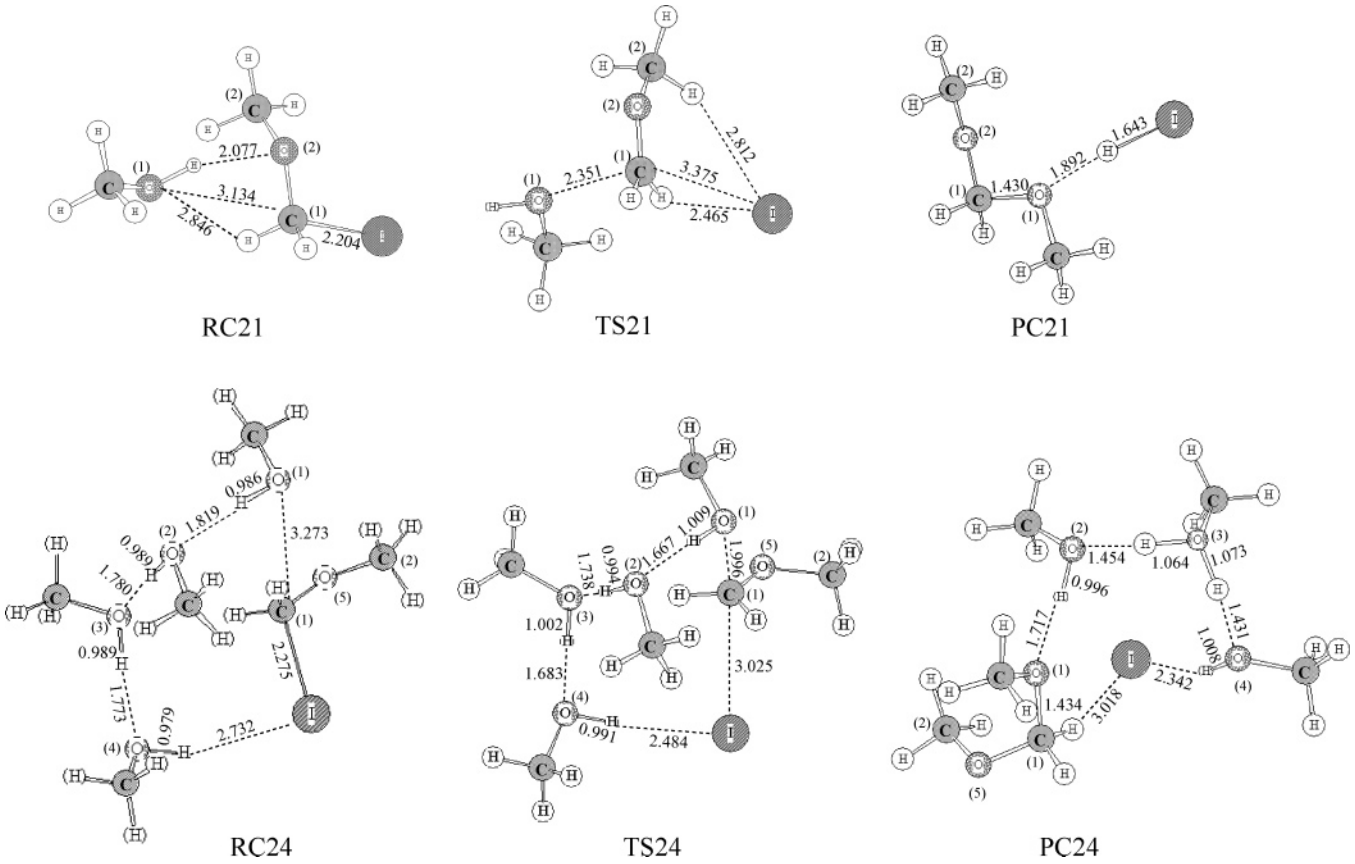

FIGURE 4. Simple schematic diagrams of the optimized structures obtained from the MP2/BS1 ab initio calculations for the reactant complexes, transition states, and product complexes of the reactions of $CH_3OCH_2I + (CH_3OH)_n \rightarrow CH_3OCH_2OCH_3 + HI + (CH_3OH)_{n-1}$ where $n = 1$ and 4. Structures for $n = 2$ and $n = 3$ can be seen in Figure S3 in the Supporting Information. See text for more details.

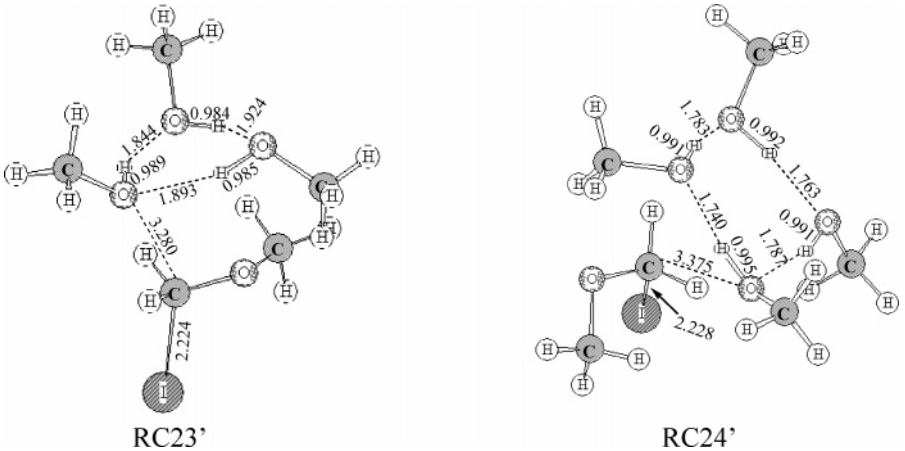

FIGURE 5. Simple schematic diagrams of the optimized structures obtained from the MP2/BS1 ab initio calculations for the reactant complexes RC23′ and RC24′ with cyclic methanol cluster structure. See text for more details.

The structure of the methanol oligomers has been investigated by some researchers.[24−29] The most stable conformation of the trimer is a cyclic chain where three O−H bonds are connected by hydrogen bonding (see T1 and T2 in Figure 1 of ref 28).[27,28] The open-chain structure of the methanol trimer (see T3 in Figure 1 of ref 28) is computed to be 3.1 kcal/mol higher in energy than T1 at the B3LYP/6-311++G(d,p) (without ZPE correction) level and to be 2.9 kcal/mol (with ZPE correction) higher at the MP2/BS1 level here. The methanol tetramer has been

(24) Buck, U.; Siebers, J.-G.; Wheatley, R. J. *J. Chem. Phys*. **1998**, *108*, 20.
(25) Provencal, R. A.; Paul, J. B.; Roth, K.; Chapo, C.; Casaes, R. N.; Saykally, R. J.; Tschumper, G. S.; Schaefer, H. F., III. *J. Chem. Phys*. **1999**, *110*, 4258.
(26) Kirschner, K. N.; Woods, R. J. *J. Phys. Chem. A* **2001**, *105*, 4150.
(27) Huisken, F.; Kaloudis, M.; Koch, M.; Werhahn, O. *J. Chem. Phys.* **1996**, *105*, 8965.
(28) Mandado, M.; Graña, A. M.; Mosquera, R. A. *Chem. Phys. Lett.* **2003**, *381*, 22.
(29) Vener, M. V.; Sauera, J. *J. Chem. Phys.* **2001**, *114*, 2623.

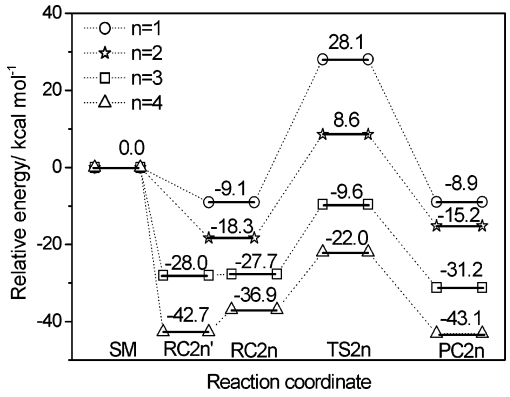

FIGURE 6. Schematic diagram depicting the MP2/BS1 calculated relative energies (in kcal/mol) for selected key reactants, transition states, and products for the reactions of $CH_3OCH_2I + (CH_3OH)_n \rightarrow CH_3OCH_2OCH_3 + HI + (CH_3OH)_{n-1}$ where $n = 1$, 2, 3, and 4. See text for more details.

TABLE 3. NBO Charges on the Approaching O(1) Atom, Leaving the I Atom, and the Center C(1) Atom for the Reaction 2 from the MP2/BS1 Computations

O(1)	$n = 1$	$n = 2$	$n = 3$	$n = 4$
reactant complex (RC)	−0.859	−0.895	−0.887	−0.885
transition state (TS)	−0.867	−0.810	−0.844	−0.851
product complex (PC)	−0.739	−0.741	−0.751	−0.753
$Q_{TS} - Q_{RC}$	−0.008	0.085	0.043	0.034
$Q_{PC} - Q_{TS}$	0.128	0.069	0.093	0.098
I	$n = 1$	$n = 2$	$n = 3$	$n = 4$
reactant complex (RC)	0.004	−0.114	−0.094	−0.137
transition state (TS)	−0.871	−0.841	−0.810	−0.821
product complex (PC)	−0.133	−0.662	−0.719	−0.856
$Q_{TS} - Q_{RC}$	−0.875	−0.727	−0.716	−0.684
$Q_{PC} - Q_{TS}$	0.738	0.179	0.091	−0.035
C(1)	$n = 1$	$n = 2$	n = 3	$n = 4$
reactant complex (RC)	−0.165	−0.083	−0.086	−0.059
transition state (TS)	0.510	0.420	0.414	0.417
product complex (PC)	0.353	0.340	0.334	0.336
$Q_{TS} - Q_{RC}$	0.675	0.503	0.500	0.476
$Q_{PC} - Q_{TS}$	−0.157	−0.080	−0.080	−0.081

previously investigated at the MP2 and DFT levels of theory,[29] and this work found that the global minimum of the methanol tetramer has an S_4 symmetry that displays a cyclic H-bonding chain and the methyl groups in an up−down, up−down configuration with respect to the H-bonding plane. We have also found an open-chain tetramer, which is 6.8 kcal/mol higher in energy than the S_4 structure obtained with the MP2/BS1 level of theory. The methanol trimer and tetramer moieties in RC23′ and RC24′ (shown in Figure 5) display cyclic configurations, as located in ref 28 and 29, and the cyclic trimer and tetramer do not interact with the iodoether through H bonding. While in RC23 and RC24, the methanol trimer and tetramer display the open-chain form. When RC23′ rearranges to RC23, the C−I bond elongates from 2.224 to 2.257 Å because of the stronger interaction of OH···I, and from RC24′ to RC24, the C−I bond elongates from 2.228 to 2.275 Å.

TABLE 4. Relative Energies and Free Energies (in kcal/mol) of the Reactants, RCs, TSs, and PCs of Reaction 2 in the MP2/BS1 and MP2/BS2 Levels[a,b]

		SM	RC2n	RC2n'	TS2n	PC2n
$n = 1$	BS1, ΔE	0.0	−9.1		28.1	−8.9
	BS1, ΔG	0.0	−1.1		37.7	0.0
	BS2, ΔE	0.0	−8.9		26.3	
	BS2, ΔG	0.0	−1.0		35.9	
$n = 2$	BS1, ΔE	0.0	−18.3		8.6	−15.2
	BS1, ΔG	0.0	−0.3		28.5	5.5
	BS2, ΔE	0.0	−18.3		6.9	
	BS2, ΔG	0.0	−0.3		26.8	
$n = 3$	BS1, ΔE	0.0	−27.7	−28.0	−9.6	−31.2
	BS1, ΔG	0.0	0.2	0.9	20.1	−0.1
	BS2, ΔE	0.0	−27.9	−26.5	−10.1	
	BS2, ΔG	0.0	0.0	2.4	19.7	
$n = 4$	BS1, ΔE	0.0	−36.9	−42.7	−22.0	−43.1
	BS1, ΔG	0.0	−0.9	−3.5	18.1	−1.9
	BS2, ΔE	0.0	−36.5	−40.4	−22.3	
	BS2, ΔG	0.0	−0.4	−1.2	17.8	

[a] SM = $CH_3OCH_2I + (CH_3OH)_n$. [b] Note: The methanol trimer and tetramer moieties in RC23′ and RC24′ (shown in Figure 5) display cyclic configurations, as located in ref 28 and 29, and the cyclic trimer and tetramer do not interact with the iodoether through H bonding. RC2n, TS2n, and PC2n denote the structures (see Figure 4 and Supporting Information Figure S3) obtained for the reactant complexes, transition states, and product complexes for reaction 2 where $n = 1$, 2, 3, and 4 is the number of additional CH_3OH molecules incorporated into the reaction systems.

The stabilization energy for RC23 is only 0.3 kcal/mol higher than that for RC23′ at the MP2/BS1 level of theory and 1.4 kcal/mol lower at the MP2/BS2 level of theory (see Table 4).

The stabilization free energy for RC23 is 0.7 and 2.4 kcal/mol lower than that for RC23′ at the BS1 and BS2 levels, respectively. The trimerization energy for the cyclic methanol trimer is 17.4 kcal/mol, and for the open-chain trimer, it is 14.5 kcal/mol; the stabilized energy for RC23 and RC23′ is 28.0 and 27.7 kcal/mol at the MP2/BS1 level. This indicates that when RC23′ rearranges to RC23 the interaction energy between the iodoether and the methanol trimer increases from 10.6 to 13.2 kcal/mol. This is similar to the $n = 4$ case. The tetramerization energy for the S_4 structure is 31.5 kcal/mol, and for the open-chain structure, it is 24.7 kcal/mol; the stabilized energy for RC24 and RC24′ is 42.7 and 36.9 kcal/mol. The interaction energy between the iodoether and the methanol tetramer increases from 11.2 to 12.2 kcal/mol. That is, to act as an acid catalyst for the leaving I atom, the methanol trimer and tetramer should rearrange to open chains to allow better interaction with the I atom, which leads to the increase in the C(1)−I bond length.

RC23 and RC24 would undergo S_N2 reactions via TS23 and TS24, respectively, which display cyclic characters similar to those of TS22. The C(1)···O(1) and C(1)···I distances in TS23 are 1.964 and 3.028 Å, respectively, and are 1.996 and 3.025 Å in TS24. The increase of the O−H bond length and the decrease in O···H distance indicate that the H transfers are also accompanied by the nucleophilic displacements. When the TS24 proceeds to PC24, the zwitterionic product $CH_3OH_2^+\cdots I^-$ is also obtained. NBO analysis (Table 2) shows $(Q_{TS} - Q_{RC})_I$ decreases from −0.727 for $n = 2$ to −0.684 for $n = 4$, and $(Q_{TS} - Q_{RC})_{O(1)}$ also decreases from 0.085 for $n = 2$ to

0.034 for $n = 4$. The $(Q_{TS} - Q_{RC})_{C(1)}$ changes slightly. These changes indicate that the charge transfers from O(1) to C(1) and from C(1) to I are both stabilized by addition of more methanol molecules in the chain. The additional methanol molecules in the chains serve as an acid catalyst for the leaving I atom and as a basic catalyst to the attacking methanol.

From the previous results, we may summarize the features of the S_N2 reaction of CH_3OCH_2I with methanol trimer/tetramer as follows: First, there may be a rearrangement of the cyclic methanol trimer/tetramer to an open-chain structure to achieve a stronger interaction with the CH_3OCH_2I substrate. Then, the O(1) atom attacks C(1) and the C(1)−I bond is induced to have some cleavage along the O(1)···C(1)···I direction, accompanied by the transfer of the H atom through the hydrogen-bonding chain. The hydrogen-bonding chain and the O(1)···C(1)···I axis form a large cyclic transition state. The final product contains a $CH_3OH_2^+\cdots I^-$ ion pair.

C. Kinetics Data Computation of Reaction 2: Large Acceleration by the Methanol Tetramer Compared to the Uncatalyzed System. To determine the contribution of the methanol clusters with different numbers of methanol molecules during the molecule−molecule S_N2 reaction in a methanol solution, the different reaction rates of CH_3OCH_2I with $(CH_3OH)_n$ were estimated.[13,18,30] Because of the very low concentration of the methoxide ion in pure methanol (ca. 10^{-9} mol/L)[31] and the relatively high activated free energy (up to 10.6 kcal/mol for $n = 3$ in the MP2/BS1 level), we may rule out the pathway of reaction 1 in this system and focus on reaction 2. We denote r_2 and r_{2n} as the total reaction rate of reaction 2 and the reaction rate that occurs via RC2n and its corresponding TS2n. According to transition-state theory, the rate constant can be calculated from the activated free energy by

$$k_{2n} = \frac{k_B T}{h} \exp\left(-\frac{\Delta G_{2n}^{\ddagger}}{RT}\right) \quad \text{(i)}$$

On the other hand, r_{2n} depends on the concentration of RC2n, which can be calculated from the stabilization energy by

$$\frac{[\text{RC2}n]}{[\text{iodoether}][\text{CH}_3\text{OH}]^n} = \exp\left(-\frac{\Delta G_{\text{RC2}n}}{RT}\right) \quad \text{(ii)}$$

where [iodoether] and $[CH_3OH]$ are the concentration of free iodoether and the methanol monomer, respectively. Obviously, [iodoether] + $\sum$[RC2n] = C_{solute}, which is the analytical concentration of iodoether. If we combine the previous two equations, we have

$$r_{2n} = k_{2n}[\text{RC2}n] = \frac{k_B T}{h}[\text{iodoether}][\text{CH}_3\text{OH}]^n \times \exp\left(-\frac{\Delta G_{2n}^{\ddagger}}{RT} - \frac{\Delta G_{\text{RC2}n}}{RT}\right) = k'_{2n}[\text{iodoether}] \quad \text{(iii)}$$

where

$$k'_{2n} \equiv \frac{k_B T}{h}[\text{CH}_3\text{OH}]^n \exp\left(-\frac{\Delta G_{2n}^{\ddagger}}{RT} - \frac{\Delta G_{\text{RC2}n}}{RT}\right) \quad \text{(iv)}$$

One may notice that k'_{2n} depends on the concentration of the methanol monomer $[CH_3OH]$ in the bulk methanol. From k'_{2n}, the relative reaction rate via different RCs can be found. To obtain $[CH_3OH]$, we also used the MP2/BS1 optimization with MP2/aug-cc-pvdz single-point computations to obtain the ΔG of $(CH_3OH)_n$ formed from n CH_3OH molecules. These ΔG values are very close to those obtained previously at the G3MP2 level of theory, and this indicates that our method for obtaining the thermodynamic data is likely reliable because the G3MP2 method is an accurate one for the calculation of thermodynamic data.[18] The results from the kinetics calculations are listed in Table 5.

The concentration of each methanol oligomer is determined by the following equations:

$$[(\text{CH}_3\text{OH})_n]/[\text{CH}_3\text{OH}]^n = \exp\left(-\frac{\Delta G_{\text{olig}}}{RT}\right) \quad \text{(v)}$$

and

$$\sum[(\text{CH}_3\text{OH})_n] = C_{\text{MeOH}} \quad \text{(vi)}$$

where C_{MeOH} is the analytical concentration of pure methanol. We can also determine [iodoether] through the following equation:

$$[\text{iodoether}]\left\{1 + \sum \exp\left(-\frac{\Delta G_{\text{RC2}n}}{RT}\right)[\text{CH}_3\text{OH}]^n\right\} = C_{\text{solute}} \quad \text{(vii)}$$

Therefore, the overall reaction rate r_2 and the pseudo-first-order rate constant can be determined by

$$r_2 = \sum r_{2n} = \sum k'_{2n}[\text{iodoether}] = \frac{\frac{k_B T}{h}[\text{CH}_3\text{OH}]^n \exp\left(-\frac{\Delta G_{2n}^{\ddagger}}{RT} - \frac{\Delta G_{\text{RC2}n}}{RT}\right)}{1 + \sum \exp\left(-\frac{\Delta G_{\text{RC2}n}}{RT}\right)[\text{CH}_3\text{OH}]^n} * C_{\text{solute}} \quad \text{(viii)}$$

$$k_2 = \frac{\frac{k_B T}{h}[\text{CH}_3\text{OH}]^n \exp\left(-\frac{\Delta G_{2n}^{\ddagger}}{RT} - \frac{\Delta G_{\text{RC2}n}}{RT}\right)}{1 + \sum \exp\left(-\frac{\Delta G_{\text{RC2}n}}{RT}\right)[\text{CH}_3\text{OH}]^n} \quad \text{(ix)}$$

Provencal, Saykally, Schaeffer, and co-workers[25] have used infrared cavity-ringdown laser absorption spectroscopy (IR−CRLAS) to study methanol clusters and found that, in high methanol concentrations, the strongest feature for O−H vibration is from the methanol tetramer. There is no observable methanol pentamer feature analogous to that of the water pentamer. They point out that the methanol tetramer may be the most important structural element in bulk methanol. Furthermore, the

(30) Wolfe, S.; Kim, C. K.; Yang, K.; Weinberg, N.; Shi, Z. *J. Am. Chem. Soc.* **1995**, *117*, 4240.

(31) Xing, Q. Y.; Xu, R. Q.; Zhou, Z.; Fei, W. W. In *Basis Organic Chemistry,* 2nd ed.; Higher Education Press of China: Beijing, China, 1993.

(32) Tashiro, M.; Stuchebrukhov, A. A. *J. Phys. Chem. B* **2005**, *109*, 1015.

TABLE 5. Concentration of Methanol Oligomers in Pure Methanol Computed in the MP2/aug-cc-pvdz and G3MP2 Levels[a]

	ΔG^{MP2}	C^{MP2}	ΔG^{G3MP2}	C^{G3MP2}
monomer	0.000	3.608	0.000	2.986
linear dimer	3.107	0.069	2.006	0.302
cyclic trimer	3.144	0.233	2.971	0.177
open trimer	4.730	0.016	4.300	0.019
cyclic tetramer	1.101	26.431	0.643	26.872
open tetramer	5.430	0.018	4.939	0.019
total		30.375		30.375

[a] Methanol clusters larger than pentamer and other conformations are neglected. Units: ΔG, kcal/mol; C, mol/L.

TABLE 6. Contribution to the Total S_N2 Reactions via Different Reactant Complexes of Reaction 2

	ΔG_{RC2n}	$\Delta G_{2n}^{\ddagger,MP2}$	k_{2n}	k_{2n}'
$n = 1$	−0.95	36.89	5.59×10^{-15}	1.01×10^{-13}
$n = 2$	−0.26	27.04	9.41×10^{-8}	1.91×10^{-6}
$n = 3$	−0.01	19.69	0.023	1.09
$n = 4$	−0.44	18.25	0.259	92.3

MP2 computation on the reaction system of iodoether and the methanol pentamer was not feasible with our current resources and was not done in our present study.

Table 6 lists the k_{2n} and k'_{2n} with different n ($n \leq 4$) values, which shows more than 98% of reaction 2 occurs via RC24. The ΔG_{RC2n} and $\Delta G_{2n}^{\ddagger}$ are obtained from MP2/BS1 optimization and MP2/BS2 single-point calculations. Compared to the uncatalyzed system (the reaction via RC21), the methanol tetramer will accelerate this reaction by about 10^{15} times, from which we can see the importance of the H-bonding chain in the S_N2 reactions of iodoether in methanol solvent. Our computations suggest that the reaction of iodoether with the methanol tetramer may be responsible for much of the observed reaction of iodoether with methanol to produce a dimethoxymethane product. We note that reaction of iodoether with the methanol tetramer will also produce a HI product (or a $CH_3OH_2^+\cdots I^-$ ion pair), whereas the S_N2 reaction of iodoether with a methoxide ion does not. We previously observed that reaction of iodoether with methanol produces some acid,[20b] and the reaction of iodoether with the methanol tetramer via an S_N2 molecule−molecule displacement reaction can probably explain this observation.

S_N2 reactions are of importance in organic reactions, and protic organic solvents such as methanol, ethanol, and *t*-butonal are often used in fundamental investigations and organic synthesis. Thus, it is of great significance to better understand the solvation effect of protic organic solvents on S_N2 reactions. In previous work, we have performed computational studies on water-catalyzed OH insertion/HX elimination reactions as well as decomposition reactions of halogenated methanols, halogenated formaldehydes, and halogenated formic acids.[16−19] In these reactions, even the existence of one H_2O molecule will greatly accelerate the reaction rates (lowering the reaction barriers). As more H_2O molecules are incorporated into the system, the reaction barriers will further decrease, but not as efficiently as the first H_2O molecule. We have also recently done similar computations for the methanol-catalyzed CH_3O insertion/HI elimination reaction with isodiiodomethane.[20a] The catalytic efficiency of methanol was observed to be lower than that of water. The solvent incorporated S_N2 reactions examined here seem a bit more complex than the HX elimination reactions[16−20] because there are more bond formations and cleavage processes are present in the S_N2 reactions, as shown in the two cases described in the preceding sections. The water/alcohol incorporated reactions may contribute significantly to a large range of reactions involving halogenated organic compounds in protic solvents such as water and methanol as well as in some basic reaction mechanisms that occur in protic solvents.

Conclusions

The MP2 method has been employed to explore the nucleophilic displacement reactions of CH_3OCH_2I with the methoxide ion and the methanol molecule, which can be representative of anion−molecule and molecule−molecule types of nucleophilic displacement reactions. For the anion−molecule type of S_N2 reaction, the incorporation of methanol molecules for better solvation of the anionic nucleophile (CH_3O^- in this paper) will increase the reaction energy barrier because of a relatively more localized charge on the nucleophiles in the reaction complexes than in the transition states. This leads to better stabilization of the RCs than the TSs by the solvent molecules. For the molecule−molecule type of S_N2 reaction, the solvation of the neutral molecular nucleophile (CH_3OH in this paper) will decrease the reaction barrier. As additional methanol molecules are incorporated in the reaction system, this reaction is inclined to proceed via a cyclic transition state where the nucleophile (CH_3**O**H) and the nucleofuge (**I**) are connected through a H-bonding chain. The nucleophilic displacements in this case are accompanied by proton transfer through the H-bonding chain. The H-bonding entities serve as both acid and base catalysts for the molecule−molecule displacement reaction. Kinetic data computed for reaction 2 indicate that the reaction via the reactant complex containing the iodoether with a methanol tetramer (RC24) contributes the most to the total reaction taking place and has a reaction rate ca. 10^{15}-fold of the uncatalyzed system.

The ab initio computation of methanol-solvated X^- + RY and X + RY reactions helps us better understand how the individual protic solvent molecules are coupled to the S_N2 reactions. Our results suggest that molecule−molecule S_N2 reactions could be very fast in methanol solutions via reaction with the methanol tetramer. Further work on related reactions in methanol solutions where the explicit consideration of the methanol molecules is done should prove an interesting area to explore. It would also be interesting to examine larger systems that have H-transfer reactions.

Acknowledgment. This research has been supported by grants from the Research Grants Council of Hong Kong (HKU/7021/03P) to D.L.P.

Supporting Information Available: Schematic diagrams (Figures S1−S3) for the optimized structures of the reactants, transition states, and products for the reactions investigated here computed from the ab initio calculations. Selected output from the ab initio calculations showing the Cartesian coordinates, total energies, and vibrational zero-point energies for the reactants, transition states, and products for the reactions investigated here. This material is available free of charge via the Internet at http://pubs.acs.org.

JO051280+